

Fabrication of three-dimensional plasmonic cavity by femtosecond laser-induced forward transfer

Wei Ting Chen,¹ Ming Lun Tseng,¹ Chun Yen Liao,² Pin Chieh Wu,¹ Shulin Sun,^{2,3} Yao-Wei Huang,¹ Chia Min Chang,⁴ Chung Hao Lu,¹ Lei Zhou,⁵ Ding-Wei Huang,⁴ Ai Qun Liu,⁶ and Din Ping Tsai^{1,2,7,*}

¹ Graduate Institute of Applied Physics, National Taiwan University, Taipei 106, Taiwan

² Department of Physics, National Taiwan University, Taipei 106, Taiwan

³ National Center of Theoretical Sciences at Taipei, Physics Division, National Taiwan University, Taipei 106, Taiwan

⁴ Graduate Institute of Photonics and Optoelectronics, National Taiwan University, Taipei 106, Taiwan

⁵ State Key Laboratory of Surface Physics and Key Laboratory of Micro and Nano Photonic Structures (Ministry of Education), Fudan University, Shanghai 200433, China

⁶ School of Electrical and Electronic Engineering, Nanyang Technological University, Singapore 639798, Singapore

⁷ Research Center for Applied Sciences, Academia Sinica, Taipei 115, Taiwan

*dptsai@phys.ntu.edu.tw

Abstract: We fabricated a three-dimensional five-layered plasmonic resonant cavity by low-cost, efficient and high-throughput femtosecond laser-induced forward transfer (fs-LIFT) technique. The fabricated cavity was characterized by optical measurements, showing two different cavity modes within the measured wavelength region which is in good agreement with numerical simulations. The mode volume corresponding to each resonance is found to be squeezed over 10^4 smaller than the cube of incident wavelength. This property may facilitate many applications in integrated optics, optical nonlinearities, and luminescence enhancement, *etc.*

© 2013 Optical Society of America

OCIS codes: (140.3390) Laser materials processing; (220.4241) Nanostructure fabrication; (160.3918) Metamaterials; (240.6680) Surface plasmons; (140.4780) Optical resonators; (250.5403) Plasmonics

References and links

1. Y. Akahane, M. Mochizuki, T. Asano, Y. Tanaka, and S. Noda, "Design of a channel drop filter by using a donor-type cavity with high-quality factor in a two-dimensional photonic crystal slab," *Appl. Phys. Lett.* **82**(9), 1341–1343 (2003).
2. T. Gu, S. Kocaman, X. Yang, J. F. McMillan, M. B. Yu, G. Q. Lo, D. L. Kwong, and C. W. Wong, "Deterministic integrated tuning of multi-cavity resonances and phase for slow-light in coupled photonic crystal cavities," *Appl. Phys. Lett.* **98**(12), 121103 (2011).
3. M. A. Noginov, G. Zhu, A. M. Belgrave, R. Bakker, V. M. Shalaev, E. E. Narimanov, S. Stout, E. Herz, T. Suteewong, and U. Wiesner, "Demonstration of a spaser-based nanolaser," *Nature* **460**(7259), 1110–1112 (2009).
4. M. H. Huang, S. Mao, H. Feick, H. Q. Yan, Y. Y. Wu, H. Kind, E. Weber, R. Russo, and P. D. Yang, "Room-temperature ultraviolet nanowire nanolasers," *Science* **292**(5523), 1897–1899 (2001).
5. D. M. Bagnall, B. Ullrich, H. Sakai, and Y. Segawa, "Micro-cavity lasing of optically excited CdS thin films at room temperature," *J. Cryst. Growth* **214**, 1015–1018 (2000).
6. S. M. Spillane, T. J. Kippenberg, and K. J. Vahala, "Ultralow-threshold Raman laser using a spherical dielectric microcavity," *Nature* **415**(6872), 621–623 (2002).
7. H. Saito, K. Nishi, I. Ogura, S. Sugou, and Y. Sugimoto, "Room-temperature lasing operation of a quantum-dot vertical-cavity surface-emitting laser," *Appl. Phys. Lett.* **69**(21), 3140–3142 (1996).
8. E. F. Schubert, A. M. Vredenberg, N. E. J. Hunt, Y. H. Wong, P. C. Becker, J. M. Poate, D. C. Jacobson, L. C. Feldman, and G. J. Zydzik, "Giant enhancement of luminescence intensity in Er-doped Si/SiO₂ resonant cavities," *Appl. Phys. Lett.* **61**(12), 1381–1383 (1992).
9. K. Tanaka, E. Plum, J. Y. Ou, T. Uchino, and N. I. Zheludev, "Multifold enhancement of quantum dot luminescence in plasmonic metamaterials," *Phys. Rev. Lett.* **105**(22), 227403 (2010).
10. J. S. Xia, Y. Ikegami, Y. Shiraki, N. Usami, and Y. Nakata, "Strong resonant luminescence from Ge quantum dots in photonic crystal microcavity at room temperature," *Appl. Phys. Lett.* **89**(20), 201102 (2006).

11. V. S. Ilchenko, A. A. Savchenkov, A. B. Matsko, and L. Maleki, "Nonlinear optics and crystalline whispering gallery mode cavities," *Phys. Rev. Lett.* **92**(4), 043903 (2004).
12. M. Soljacic and J. D. Joannopoulos, "Enhancement of nonlinear effects using photonic crystals," *Nat. Mater.* **3**(4), 211–219 (2004).
13. D. K. Armani, T. J. Kippenberg, S. M. Spillane, and K. J. Vahala, "Ultra-high-Q toroid microcavity on a chip," *Nature* **421**(6926), 925–928 (2003).
14. M. T. Hill, Y. S. Oei, B. Smalbrugge, Y. Zhu, T. De Vries, P. J. Van Veldhoven, F. W. M. Van Otten, T. J. Eijkemans, J. P. Turkiewicz, H. De Waardt, E. J. Geluk, S. H. Kwon, Y. H. Lee, R. Notzel, and M. K. Smit, "Lasing in metallic-coated nanocavities," *Nat. Photonics* **1**(10), 589–594 (2007).
15. M. P. Nezhad, A. Simic, O. Bondarenko, B. Slutsky, A. Mizrahi, L. A. Feng, V. Lomakin, and Y. Fainman, "Room-temperature subwavelength metallo-dielectric lasers," *Nat. Photonics* **4**(6), 395–399 (2010).
16. K. Yu, A. Lakhani, and M. C. Wu, "Subwavelength metal-optic semiconductor nanopatch lasers," *Opt. Express* **18**(9), 8790–8799 (2010).
17. S. Noda, K. Tomoda, N. Yamamoto, and A. Chutinan, "Full three-dimensional photonic bandgap crystals at near-infrared wavelengths," *Science* **289**(5479), 604–606 (2000).
18. Y. Akahane, T. Asano, B. S. Song, and S. Noda, "High-Q photonic nanocavity in a two-dimensional photonic crystal," *Nature* **425**(6961), 944–947 (2003).
19. K. J. Vahala, "Optical microcavities," *Nature* **424**(6950), 839–846 (2003).
20. R. F. Oulton, V. J. Sorger, T. Zentgraf, R. M. Ma, C. Gladden, L. Dai, G. Bartal, and X. Zhang, "Plasmon lasers at deep subwavelength scale," *Nature* **461**(7264), 629–632 (2009).
21. S. A. Maier, P. G. Kik, H. A. Atwater, S. Meltzer, E. Harel, B. E. Koel, and A. A. G. Requicha, "Local detection of electromagnetic energy transport below the diffraction limit in metal nanoparticle plasmon waveguides," *Nat. Mater.* **2**(4), 229–232 (2003).
22. R. Ameling and H. Giessen, "Microcavity plasmonics: strong coupling of photonic cavities and plasmons," *Laser Photonics Rev.* 1–29 (2012) / DOI 10.1002/lpor.201100041.
23. S. Larouche, Y.-J. Tsai, T. Tyler, N. M. Jokerst, and D. R. Smith, "Infrared metamaterial phase holograms," *Nat. Mater.* **11**(5), 450–454 (2012).
24. W. T. Chen, C. J. Chen, P. C. Wu, S. Sun, L. Zhou, G.-Y. Guo, C. T. Hsiao, K.-Y. Yang, N. I. Zheludev, and D. P. Tsai, "Optical magnetic response in three-dimensional metamaterial of upright plasmonic meta-molecules," *Opt. Express* **19**(13), 12837–12842 (2011).
25. P. C. Wu, W. T. Chen, K.-Y. Yang, C. T. Hsiao, G. Sun, A. Q. Liu, N. I. Zheludev, and D. P. Tsai, "Magnetic plasmon induced transparency in three-dimensional metamolecules," *Nanophoton.* **1**, 131–138 (2012).
26. S. Juodkazis, V. Mizeikis, and H. Misawa, "Three-dimensional microfabrication of materials by femtosecond lasers for photonics applications," *J. Appl. Phys.* **106**(5), 051101 (2009).
27. M. Malinauskas, P. Danilevičius, and S. Juodkazis, "Three-dimensional micro-/nano-structuring via direct write polymerization with picosecond laser pulses," *Opt. Express* **19**(6), 5602–5610 (2011).
28. A. Vailionis, E. G. Gamaly, V. Mizeikis, W. Yang, A. V. Rode, and S. Juodkazis, "Evidence of superdense aluminium synthesized by ultrafast microexplosion," *Nat Commun* **2**, 445 (2011).
29. C. M. Chang, M. L. Tseng, B. H. Cheng, C. H. C. Y. Z. Ho, H. W. Huang, Y.-C. Lan, D.-W. Huang, A. Q. Liu, and D. P. Tsai, "Three-dimensional plasmonic micro projector for light manipulation," *Adv. Mater.* (2012) / DOI: 10.1002/adma.201203308.
30. M. L. Tseng, Y.-W. Huang, M.-K. Hsiao, H. W. Huang, H. M. Chen, Y. L. Chen, C. H. Chu, N.-N. Chu, Y. J. He, C. M. Chang, W. C. Lin, D.-W. Huang, H.-P. Chiang, R.-S. Liu, G. Sun, and D. P. Tsai, "Fast fabrication of a Ag nanostructure substrate using the femtosecond laser for broad-band and tunable plasmonic enhancement," *ACS Nano* **6**(6), 5190–5197 (2012).
31. C. H. Chu, C. D. Shiue, H. W. Cheng, M. L. Tseng, H.-P. Chiang, M. Mansuripur, and D. P. Tsai, "Laser-induced phase transitions of Ge₂Sb₂Te₅ thin films used in optical and electronic data storage and in thermal lithography," *Opt. Express* **18**(17), 18383–18393 (2010).
32. A. I. Kuznetsov, R. Kiyari, and B. N. Chichkov, "Laser fabrication of 2D and 3D metal nanoparticle structures and arrays," *Opt. Express* **18**(20), 21198–21203 (2010).
33. K. S. Kaur, A. Z. Subramanian, Y. J. Ying, D. P. Banks, M. Feinaeugle, P. Horak, V. Apostolopoulos, C. L. Sones, S. Mailis, and R. W. Eason, "Waveguide mode filters fabricated using laser-induced forward transfer," *Opt. Express* **19**(10), 9814–9819 (2011).
34. A. I. Kuznetsov, A. B. Evlyukhin, M. R. Gonçalves, C. Reinhardt, A. Koroleva, M. L. Arnedillo, R. Kiyari, O. Marti, and B. N. Chichkov, "Laser fabrication of large-scale nanoparticle arrays for sensing applications," *ACS Nano* **5**(6), 4843–4849 (2011).
35. M. L. Tseng, P. C. Wu, S. Sun, C. M. Chang, W. T. Chen, C. H. Chu, P.-L. Chen, L. Zhou, D.-W. Huang, T.-J. Yen, and D. P. Tsai, "Fabrication of multilayer metamaterials by femtosecond laser-induced forward-transfer technique," *Laser Photon. Rev.* **6**(5), 702–707 (2012).
36. M. L. Tseng, C. M. Chang, B. H. Chen, Y.-W. Huang, C. H. Chu, K. S. Chung, Y. J. Liu, H. G. Tsai, N.-N. Chu, D.-W. Huang, H.-P. Chiang, and D. P. Tsai, "Fabrication of plasmonic devices using femtosecond laser-induced forward transfer technique," *Nanotechnology* **23**(44), 444013 (2012).
37. M. L. Tseng, B. H. Chen, C. H. Chu, C. M. Chang, W. C. Lin, N.-N. Chu, M. Mansuripur, A. Q. Liu, and D. P. Tsai, "Fabrication of phase-change chalcogenide Ge₂Sb₂Te₅ patterns by laser-induced forward transfer," *Opt. Express* **19**(18), 16975–16984 (2011).

38. M. Feinaeugle, A. P. Alloncle, P. Delaporte, C. L. Sones, and R. W. Eason, "Time-resolved shadowgraph imaging of femtosecond laser-induced forward transfer of solid materials," *Appl. Surf. Sci.* **258**(22), 8475–8483 (2012).
39. C. B. Arnold, P. Serra, and A. Pique, "Laser direct-write techniques for printing of complex materials," *MRS Bull.* **32**(01), 23–32 (2007).
40. M. Colina, P. Serra, J. M. Fernández-Pradas, L. Sevilla, and J. L. Morenza, "DNA deposition through laser induced forward transfer," *Biosens. Bioelectron.* **20**(8), 1638–1642 (2005).
41. J. Xu, J. Liu, D. H. Cui, M. Gerhold, A. Y. Wang, M. Nagel, and T. K. Lippert, "Laser-assisted forward transfer of multi-spectral nanocrystal quantum dot emitters," *Nanotechnology* **18**(2), 025403 (2007).
42. S. Mailis, I. Zergioti, G. Koundourakis, A. Ikiades, A. Patentalaki, P. Papakonstantinou, N. A. Vainos, and C. Fotakis, "Etching and printing of diffractive optical microstructures by a femtosecond excimer laser," *Appl. Opt.* **38**(11), 2301–2308 (1999).
43. P. B. Johnson and R. W. Christy, "Optical constants of the noble metals," *Phys. Rev. B* **6**(12), 4370–4379 (1972).
44. X. Yang, J. Yao, J. Rho, X. Yin, and X. Zhang, "Experimental realization of three-dimensional indefinite cavities at the nanoscale with anomalous scaling laws," *Nat. Photonics* **6**(7), 450–454 (2012).
45. J. Yao, X. D. Yang, X. B. Yin, G. Bartal, and X. Zhang, "Three-dimensional nanometer-scale optical cavities of indefinite medium," *Proc. Natl. Acad. Sci. U.S.A.* **108**(28), 11327–11331 (2011).
46. R. Loudon, "The propagation of electromagnetic energy through an absorbing dielectric," *J. Phys. A.* **3**(3), 233–245 (1970).
47. R. Ruppin, "Electromagnetic energy density in a dispersive and absorptive material," *Phys. Lett. A* **299**(2-3), 309–312 (2002).
48. N. R. Han, Z. C. Chen, C. S. Lim, B. Ng, and M. H. Hong, "Broadband multi-layer terahertz metamaterials fabrication and characterization on flexible substrates," *Opt. Express* **19**(8), 6990–6998 (2011).
49. D. P. Banks, C. Grivas, I. Zergioti, and R. W. Eason, "Ballistic laser-assisted solid transfer (BLAST) from a thin film precursor," *Opt. Express* **16**(5), 3249–3254 (2008).

1. Introduction

Optical cavity has found many applications in integrated photonics [1, 2], micro/nano-laser [3–7], luminescence enhancement [8–10] and nonlinear optics [11, 12]. To achieve high performances on above-mentioned applications, an optical cavity with a high Purcell factor Q/V_m is desired, where Q and V_m denotes the quality factor and mode volume. Dielectric optical cavities, such as microdisks [13], metal cladding [14–16] and photonic crystals [17, 18], typically show high quality factors (usually $> 10^3$), but, the mode volumes in these systems are limited by the diffraction limit. Moreover, dielectric cavities are too big to be integrated with electronic devices [19]. In contrast, plasmonic cavities can squeeze light in volumes significantly smaller than the diffraction limit, so that they have drawn lots of attention recently [20, 21]. To fabricate multilayer and/or three-dimensional plasmonic nanostructures, the focused ion beam (FIB) and electron beam lithography (EBL) technique are frequently adopted [22–25]. However, using above-mentioned technique, the alignment error is difficult to overcome [23] and the processing time is proportional to the number of layers in the structure. These drawbacks make the applications of EBL and FIB technique to multilayer metamaterials less attractive for industrial in-line mass production. In contrast, laser-induced forward transfer (LIFT) as a kind of laser-direct writing technique [26–31] is very useful in fabricating photonic devices because of its low costing and simple experimental setup [32–35]. Under focused laser illumination, the local material on the precoated substrate (so called donor) can be transferred to the opposite substrate (so called receiver). LIFT technique is very versatile, the processed materials can be not only solid materials [33–38] but also liquid [39], bio-materials [40], and powders [41]. In particular, we recently demonstrated that, with tightly contacted donor-receiver pair, multilayer plasmonic structures can be fabricated on donor by LIFT process [35]. Since the processing rate [34] and controllability [42] of LIFT can be much better in comparison with other maskless fabrication techniques, LIFT technique is very fascinating for the throughput and fast prototyping of various nanophotonic devices.

In this paper, we implement the femtosecond LIFT (fs-LIFT) technique to fabricate square-shaped multilayer plasmonic resonant cavities, and study their optical properties by both experiments and numerical simulations. We chose to fabricate this type of plasmonic cavity because such a system was shown to exhibit extremely small mode volume. Using the fs-LIFT technique, the illuminated materials of multilayer thin films on donor are ablated and

partially transferred to the tightly contact receiver, which would leave the uniform squared multilayer plasmonic cavities which are surrounded by the cooled-down laser-ablated materials on the donor. We found that the fabricated plasmonic cavity indeed exhibits two cavity modes with mode volume $\sim 10^{-4} \lambda^3$, which is highly desired in many applications.

2. Experimental

Figure 1 shows the schematic illustration of the experimental process. By using a magnetron sputtering system (Shibaura Mechatronics Corp.), multilayer thin films composed of Au(20 nm) / ZnS-SiO₂(30 nm) / Au(20 nm) / ZnS-SiO₂(30 nm) / Au(20 nm) are sputtered on a cleaned BK7 glass substrate (Matsunami cover glass, 22 × 22 mm², thickness = 0.15 mm) in Ar atmosphere (5×10^{-1} pa). In the fs-LIFT process, the multilayer thin films are treated as the donor. In our previous work we found, for fabricating the multilayered nanostructures using fs-laser beam, it is necessary to put another substrate on the top of the multilayered films to prevent the nonuniform edges of fabricated structures caused by laser-induced explosion [30]. Another glass substrate acting as the receiver is tightly contacted with the donor substrate. Subsequently, the donor-receiver pair is mounted on a computer controlled stage (Mad City Labs Inc., Nano-LP200). A Ti:Sapphire fs-laser laser (Coherent Inc., Chameleon ultra II, $\lambda = 800$ nm, pulse duration = 140 fs, repetition rate = 80 MHz) is used as a light source. An attenuator is used for controlling the incident laser fluence precisely. The laser beam is focused on the donor side by a high-numerical-aperture oil-immersion objective lens (Zeiss Plan-Apochromat, 100 ×, N.A. = 1.4, working distance = 0.17 mm) through the glass substrate on the donor. The illuminated materials in multilayer films are locally melted and mixed after the laser treatment. Non-illuminated parts of the laser-processed thin films are surrounded by the cool-down laser-ablated materials. Therefore, the multilayer cavities are fabricated after the fs-LIFT process with a designed laser raster path. The designed multilayer structure as single unit-cell is depicted in Fig. 1(b). The feature sizes of each a square-shaped cavity is 500 nm length and 120 nm height, and the periodicity is 1100 nm and 650 nm in *x*-direction and *y*-direction, respectively.

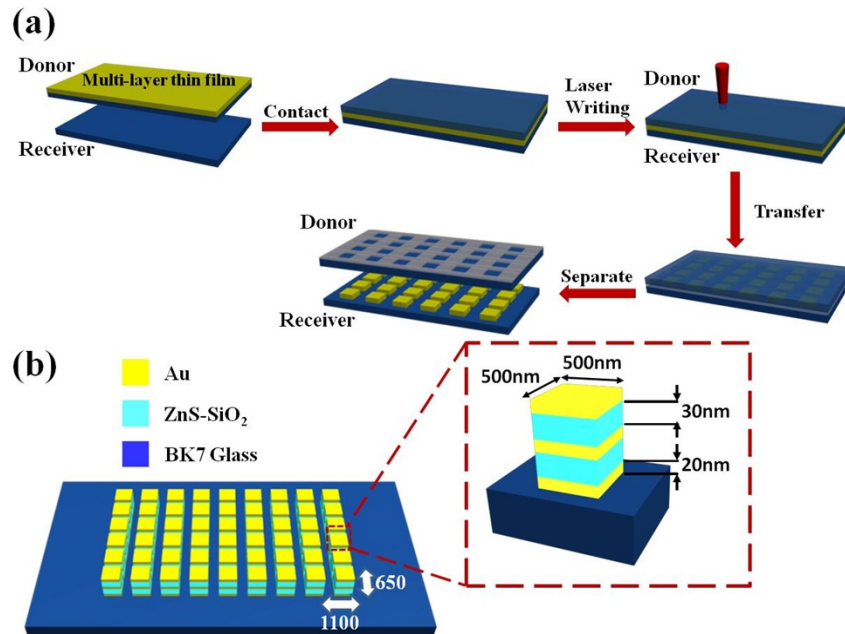


Fig. 1. (a) Schematic illustration of fs-LIFT process. (b) The feature size of a multilayered plasmonic cavity in nanometer scale. The period along *x*-direction P_x and *y*-direction P_y are 1100 nm and 650 nm.

3. Results and discussions

Figure 2(b) shows the square patterns surrounded with laser-ablated materials transferred onto the receiver (indicated with red-dashed square). The laser fluence is set at 165 mJ/cm^2 (raster speed is fixed as $53.3 \text{ } \mu\text{m/s}$). The square patterns can be transferred to receiver by the laser-ablated materials, which are impressed on the receiver during the fs-LIFT process. Moreover, as shown in the green dashed square in Fig. 2(b) and the corresponding magnified SEM image shown in Fig. 2(c), multilayer films of fabricated patterns can be observed, indicating that the multilayer structures of laser-fabricated pattern are not damaged by the lateral heat dissipation during laser illumination. Since the structures shown in Fig. 2(a) are not completed and uniform, the laser processing condition should be modified.

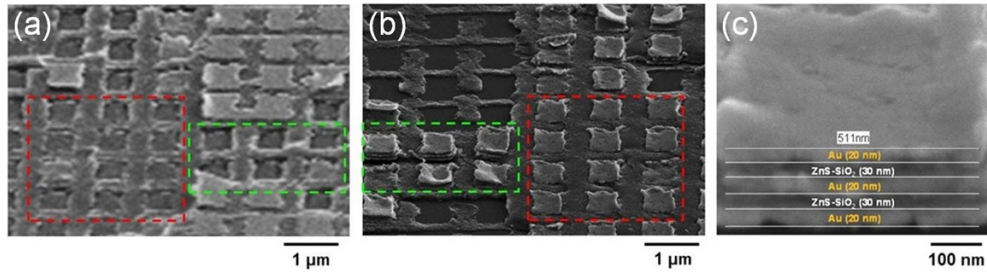


Fig. 2. SEM images of the fabricated structures on (a) donor and (b) receiver. (c) Magnified SEM image of receiver.

Figures 3(a) and 3(b) show the SEM images of the fabricated samples on the donor and corresponding receiver, respectively. The fluence of incident laser beam is increased to 170 mJ/cm^2 , and the raster speed is fixed at $53.3 \text{ } \mu\text{m/s}$. On the donor, regular square patterns which are surrounded by laser-processed materials can be observed on the surface. The SEM images show the length of such square pattern is around 500 nm . The corresponding structures on receiver show rough surface morphology and edges, indicating that the transferred structures are composed of mixed materials of multilayer films (*i.e.*, Au and ZnS-SiO₂).

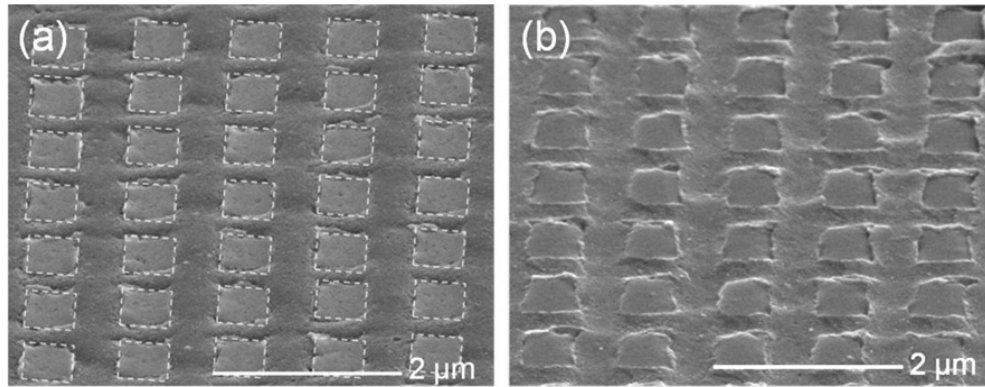


Fig. 3. SEM images of (a) the fabricated multilayer cavity arrays on donor and (b) the corresponding laser-transferred structures on receiver.

Figure 4 shows the experimental (red solid line) as well as simulated (blue solid line) transmittance spectra of the plasmonic cavity illuminated by a y -polarized light at normal-incidence. The transmittance spectra from $\lambda = 1000 \text{ nm}$ to $\lambda = 2500 \text{ nm}$ were measured using a Bruker VERTEX 70 Fourier-transform infrared spectrometer with a Bruker HYPERION 1000 infrared microscope ($15 \times$ Cassegrain objective, numerical aperture N.A. = 0.4, near-infrared polarizer, and an InGaAs and MCT detector). An iris was used to collect the incident light to a square area of about $50 \times 50 \text{ } \mu\text{m}^2$. The transmittance spectra are normalized by those

of the rare fused silica wafer. The simulation spectra were obtained by the commercial software (Comsol Multiphysics) based on the finite-element method. The dimension of simulated squared plasmonic cavity is 500 nm with its periodicity as 1100 nm and 650 nm in x- and y-direction. Periodic boundary conditions are used to mimic the plasmonic cavity array. The refractive index (n) of the sandwiched ZnS-SiO₂ layer was taken as 2.3, considering the ZnS-SiO₂ mixture made of 80% ZnS ($n = 2.5$) with 20% SiO₂ ($n = 1.5$). The permittivity of gold was described by the Drude-Lorentz model with a damping constant of 0.35 eV and a plasma frequency of 8.997 eV [43]. We found that two transmittance dips appear around 1280 nm (Mode II) and 1800 nm (Mode I) in both experimental and simulated spectra. The discrepancy between simulation and experiment is due to the fabrication defect in the sample and the inaccuracies of the dielectric parameter taken in simulations.

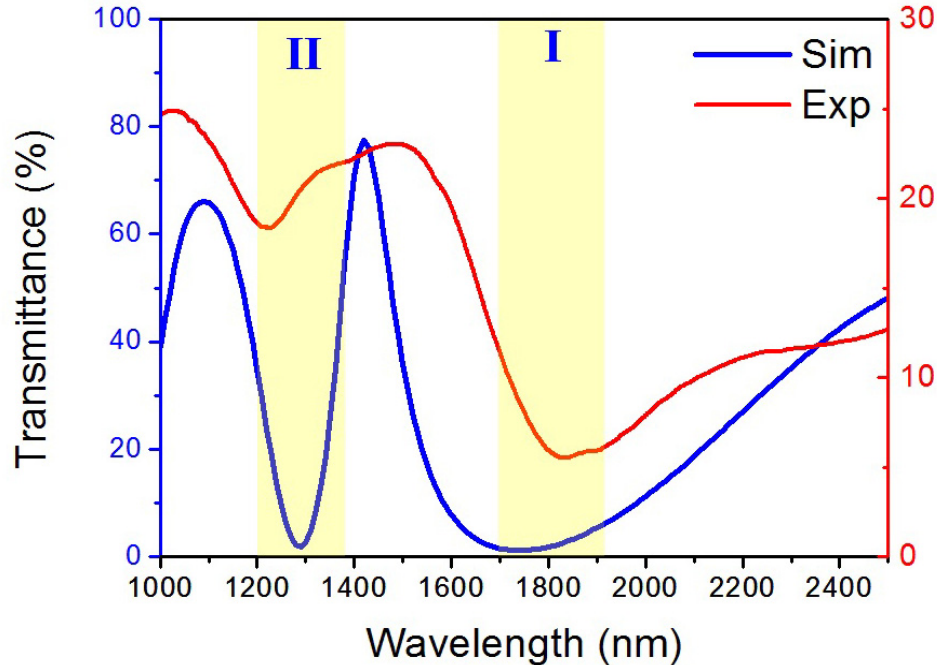


Fig. 4. A comparison transmittance spectra between experimental result (red curve) and simulation result (blue curve). Two resonance modes are marked by I and II from longer to shorter wavelength.

To understand the origin of these resonance modes, we depicted the electromagnetic field patterns for two modes in Fig. 5. To gain a complete picture of the two cavity modes, we showed the E_z field at the $y = 0$ nm plane, the E_z and H_x fields at the $z = 85$ nm plane (center symmetry plane of upper ZnS-SiO₂ layer), respectively. For mode I, half-wavelength standing wave behaviors along three dimensions demonstrate that it is the resonance mode with index (1,1,1) [44]. Recalling that the size of the plasmonic cavity is 500 nm \times 500 nm \times 120 nm, we found that such a resonance mode (with $\lambda \sim 1800$ nm) exhibits subwavelength property with high energy storage ability. Similar analysis revealed that mode II is a resonance mode with index (1,2,1). Considering the distances of plasmonic cavities are different along x and y direction, the case of electric field polarized along x direction has also been studied. It was found that the electromagnetic field distributions of the plasmonic resonant modes are similar with the above-mentioned y -polarized case due to the symmetry of square-shaped cavity, except for about 200 nm blue shift of the plasmonic resonant wavelengths.

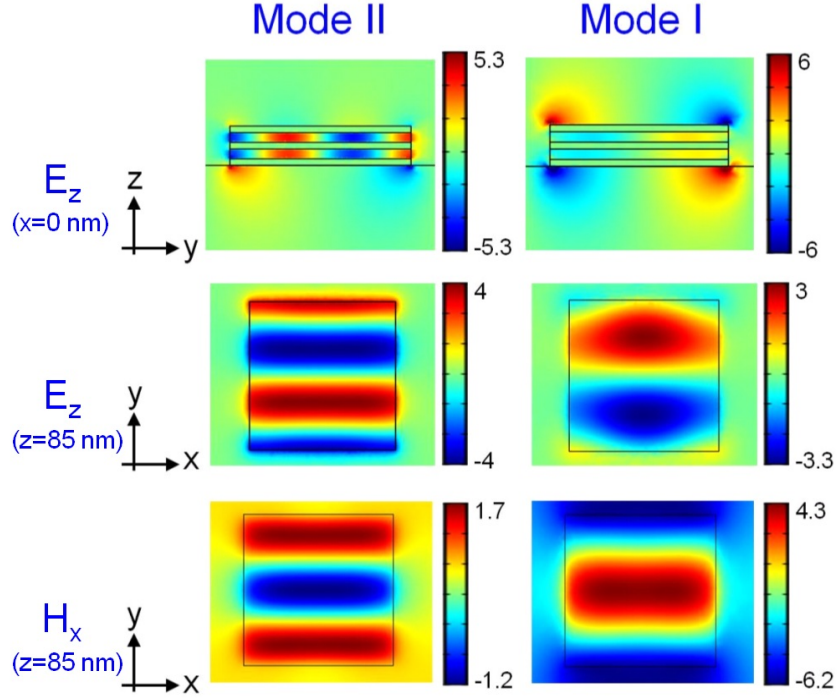


Fig. 5. Analysis of plasmonic resonance modes. The first and second column corresponds to mode II and mode I. The first row show electric field distribution of z -component (E_z) corresponding to xz plane. The second and the third row show the magnetic field of x -component (H_x) and electric field of z -component (E_z) corresponding to xy plane at height $z = 85$ nm, respectively. Colorful scale bar shows relative intensity in arbitrary unit.

For a given resonance mode, the quality factor Q is determined by the photon life time, and the mode volume V_m quantifies the electromagnetic field strength per photon. According to our simulation spectra, we calculated the quality factors of the two modes and found that they are 3.2 and 8.3, respectively. Indeed, the quality factor Q of such a plasmonic cavity is very low due to the absorption loss of metal. However, our plasmonic cavities have smaller mode volumes (V_m) compared to dielectric micro-cavities. The mode volume V_m is calculated by [44, 45]

$$V_m = \frac{1}{\max(W_{av}(\vec{r}))} \iiint W_{av}(\vec{r}) d^3 r \quad (1)$$

where W_{av} is the time averaged electromagnetic energy density calculated by [46, 47]

$$W_{av} = \frac{\epsilon_0}{4} \left(\epsilon' + \frac{2\omega\epsilon''}{\Gamma_e} \right) |E|^2 + \frac{\mu_0}{4} |H|^2 \quad (2)$$

where Γ_e , ϵ' and ϵ'' are the damping frequency, the real part and image part of permittivity. The $\max(W_{av})$ is chosen at the maximum energy density excluding the sharp peak at the corner, since it strongly depends on the mesh quality at the corner. Our calculations revealed that the mode volume V_m can go down to $1.68 \times 10^{-4} \lambda^3$ and $2.8 \times 10^{-4} \lambda^3$ for mode I, and mode II, in consistency with our expectation that a plasmonic cavity can confine electromagnetic energy far below the diffraction limit. Together with the quality factor Q of the cavity resonance, this enables Q/V_m in the case of the fs-laser fabricated multilayered plasmonic cavity to be comparable with dielectric optical cavities. Nevertheless, the multilayered plasmonic cavity fabricated by fs-LIFT has relatively smaller geometrical size,

and therefore shows the feasibility to be highly integrated in a given chip with low-cost, high throughput and efficiency.

4. Conclusion

We successfully demonstrated a low-cost, efficient and simple fabrication technique for manufacturing multilayered plasmonic resonance cavity by femtosecond laser-induced forward transfer technique. We have found the optimized laser fluence (170 mJ/cm^2) and laser raster speed ($53.3 \text{ }\mu\text{m/s}$) on the multilayer films for making the fabricated multilayer structure uniform and smooth. Two resonance modes are found in near infrared region, showing electromagnetic energy mainly stored in the sandwiched dielectric layer with subwavelength property. The optical properties of laser-fabricated plasmonic cavity quantitatively agree with simulations results. These unique properties of multilayered cavity increase the optical density of state and therefore could be applied to light-matter interactions, such as integrated optics, optical nonlinearities, and luminescence enhancement, *etc.* This work demonstrates the potential of fs-LIFT technique in fabrications of various kinds of three-dimensional nanostructures: People can readily find the optimization of processing parameters for the desired layered structures, and fabricate the designed photonic devices on the arbitrary substrates. Our strategy can be further improved by the integration with other laser-direct writing technique such as laser micro-lens array photolithography [48] and laser ablation by a laser beam of flat-top profile [49].

Acknowledgments

The authors acknowledge financial support from National Science Council, Taiwan under grant numbers 100-2923-M-002-007-MY3, 101-3113-P-002-021, 101-2112-M-002-023, 101-2911-I-002-107, and 100-2221-E-002-134, respectively. They are also grateful to National Center for Theoretical Sciences, Taipei Office, Molecular Imaging Center of National Taiwan University, National Center for High-Performance Computing, Taiwan, and Research Center for Applied Sciences, Academia Sinica, Taiwan for their support. LZ thanks financial supports from National Science Foundation of China (60990320, 60990321, 60990324, and 11174055) and Program of Shanghai Subject Chief Scientist (12XD1400700).